Development of a Two-Dimensional CFD Code to Simulation of a Flapping Foil Problem at Low Reynolds Numbers

Alireza Rezaei[1], Morteza Namvar[2], Farhad Ghadak[3]

[۱]Marine Technology Faculty, Amirkabir University of Technology, a.r.rezaei@aut.ac.ir
[۲] Aerospace Faculty, Amirkabir University of Technology, mortezanamvar@aut.ac.ir
[۳]Iranian Society of Computational Science and Engineering, F.Ghadak@chmail.ir

Abstract
A computational fluid dynamic (CFD) code has been developed for simulation of two-dimensional flapping foil problem. Viscos flow has been simulated in an arbitrary Lagrangian-Eulerian description and a high quality mesh deformation technique used for modifying of the grid structure. The abilities of code is verified in compare of other references values and a good agreement with other numerical results has been observed. Structures of vortices are simulated and effect of them in leading and trailing edge regions on the thrust generation is investigated. The mechanism of thrust generation in flapping foil is attended and observed that it works based on exhaust of momentum, look like other propulsion systems. A mean flow, which has averaged during ۲۰ period of oscillation, showed the accelerating of flow behind the foil and resemblance of the flow pattern with a jet flow. But flapping foil in contrast to jet flow has an unsteady inherent.

Keywords: Flapping foil; viscos flow; low Reynolds number

Introduction

Many of animals like insects, birds, cetaceans, fishes and … use of flapping wings to move. Both biological and engineering scientists have always been interested to detect the mystery of mechanism of this motion. For a long time, the fluid dynamic mechanism behind flapping insect flight or fish motion was a complete mystery, until several decades ago. With Experiments it has been discovered that the presence of a vortex on top of the flapping wings, generates forces larger than obtained by using conventional propulsion systems. So an efficient system of propulsion can be tabernacle with common systems. Flapping wings produce both lifting and propulsive forces. Two main and important characteristic which are needed for engineering goals. For example a micro air vehicles (MAV) and autonomous underwater vehicle (AUV) use these properties for exploration and surveillance.

In order to design and optimise MAV and AUV several flow visualisation experiments and numerical simulations have been performed to achieve a deep understanding of flapping wing aero and hydrodynamic. The effects of kinematics of wing on the flow and forces is still not fully understood and are under consideration.

A large amount of experiments and computations has been accomplished on flapping-wing related topics and many comprehensive reviews and book chapters, [۱], [۲], [۳] and [٤], have explained these works from different aspects. These topics include kinematics of flapping flight, wing/foil geometry and aero(hydro)-elasticity, multiple wing/foil configuration, unsteady flow structure analyses, especially on the wake structures, leading edge vortices (LEVs) dynamics and vortex interactions, and fluid dynamic forces and propulsion efficiency analyses, etc. Before moving forward, previous studies on some of the aforementioned topics, which will be in relation with the present paper, are briefly reviewed as follows.

It is well known that flapping motions, in comparison with jet or propeller systems, can effectively generate thrust at low and moderate Reynolds number. The explanation for the thrust generation with oscillating foils was given by Knoller [٥] and Betz [٦] independently based on the inviscid assumption and the effective angle of attack concept. This was experimentally confirmed by Katzmayr [۷] through mounting a stationary wing in an oscillating flow. After that, von Karman and Burgers [۸] showed a thought-provoking way to explain the thrust or drag production by checking momentum surfeit or deficit in the wake based on the wake vortices orientation and location. This has gradually become a qualitative principle to judge whether an oscillating mechanism generate thrust or drag. The aforementioned wake structure analyses originate from this work and have attracted intensive research attentions.

In this field, some interesting wake vortices phenomena have been observed and their impact on the fluid dynamic performance of the oscillating foils/wings has been noticed. The vortex street of the thrust-indicative type for pure heaving or pitching motion of NACA۰۰۱۵ foil, reported by Freymuth [۹]. Koochesfahani [۱۰] mentioned that by adjusting the pitching frequency, amplitude and the shape of the oscillation wave, the wake pattern after a pitching foil can be controlled. Later, the optimal thrust development in oscillating foils reported at range of ۰,۲۵ to ۰,۳۵ for Strouhal number by Triantafyllou et al. [۱۱]. With used of water-tunnel experiments and inviscid flow simulations, Jones et al. [۱۲] evaluated the wake structures behind a heaving foil. A comprehensive classification of wake types was summarized in their results. The jet characteristics behind a heaving NACA۰۰۱۲ foil with the dye flow visualization

and laser Doppler velocimetry (LDV) measurements studied by Lai and Platzer [١٣]. Wang [١٤] investigated pure heaving motion and reported a close relation between leading edge vortices (LEVs) and trailing edge vortices (TEVs). The wake patterns behind a heaving foil numerically simulated and LEVs' effects on the wake pattern and propulsive efficiency evaluated. Young and Lai [١٥] studied different types of wake structures behind a heaving foil and the associated fluid dynamic forces. They found that the fluid dynamic forces relied more on the dynamic behaviours of LEVs while the wake structures were mainly controlled by the TEVs. Schnipper et al. [١٦] performed a systematic study on the wake patterns behind a pitching foil in the vicinity of the drag-thrust transition region in order to reveal the connection between wake structures and aerodynamic force generation. As a continuation of previous work, Bohl and Koochesfahani [١٧] studied the wake structures behind a sinusoidal pitching NACA٠٠٢٠ foil of various reduced frequencies using molecular tagging velocimetry (MTV).

The present study deals with the development and improvement of computational solver to simulation of the flow around flapping wings at low Reynolds numbers. A two-dimensional numerical simulations in order to observe the wing motion and flow physics has been performed.

In first section, simulation parameters of problem, which describe its main characterises, are mentioned. Section two pays to governing equation in a fluid structure interaction problem. In section three, numerical methods, which have been adopted for spatial and temporal discretization, are discussed and radial basis function (RBF) mesh deformation method, as a high quality mesh smoothing method, is clarified. A brief mention to grid structure, which has used, and boundary conditions, which are implemented, accomplishes in Section four. Section five appertain to validation of code and verification of results and analyse of them. In the last section a brief conclusion about the work and results is presented.

١. Problem description

The foil NACA٠٠١٢ with chord length c is excited with a harmonic heaving motion $h(t)$ in a uniform flow of low speeds. The free-stream velocity and Mach number are U_∞ and M_∞. The heaving movement for the foil is described with Eq. (١):

$$h(t) = h_. \sin(\omega t) \qquad (١)$$

Where ω is the angular frequency and $h_.$ refers to heave amplitude.

The reduce frequency k is defined as Eq. (٢):

$$k = \frac{٢\pi cf}{U_\infty} \qquad (٢)$$

Where f denotes the frequency of foil oscillation in Hz. For flapping cases, the Strouhal number as a main parameter has a wide application and St is defined as:

$$St = \frac{fA}{U_\infty} \qquad (٣)$$

Where A denotes the characteristic width of the wake flow. Usually$A = ٢h_.$.

The instantaneous fluid dynamic force components $X(t)$ and $Y(t)$ are in the x-and y-directions, respectively. The corresponding non-dimensional coefficients based on the free-stream dynamic pressure and the foil chord are $cx(t)$, $cy(t)$, respectively. The instantaneous pressure coefficient is denoted as $cp(t)$.

The time-averaged value of $X(t)$ over a period of the oscillation denoted by F is the thrust generated by the foil.

$$F = -\frac{١}{T}\int_.^T X(t)dt \qquad (٤)$$

٢. Governing Equation

Within a fluid-structure interaction problem (FSI) application the computational domain is no longer fixed but changes in time, which has to be taken into account. Besides other numerical techniques, the most popular one is the so-called Arbitrary Lagrangian–Eulerian (ALE) formulation. Here the conservation equations for mass and momentum and energy, which are to be solved based on a finite-volume scheme, are re-formulated for a temporally varying domain, i.e., control volumes (CV) with time-dependent volumes V_t and surfaces S_t. Hence the governing equations in ALE formulation expressing the conservation of mass, momentum and total energy read:

$$\frac{d}{dt}\int_{V_t}\rho\,\mathrm{dV}+\int_{S_t}\rho\,(u_j-u_{gj}).n_j\,\mathrm{dS}=0 \quad (5)$$

$$\frac{d}{dt}\int_{V_t}\rho u_i\,\mathrm{dV}+\int_{S_t}\rho u_i\,(u_j-u_{gj}).n_j\,\mathrm{dS}=\int_{S_t}(\tau_{ij}+\delta_i p).n_j\,\mathrm{dS} \quad (6)$$

$$\frac{d}{dt}\int_{V_t}\rho E\,\mathrm{dV}+\int_{S_t}(\rho E+p)\,(u_j-u_{gj}).n_j\,\mathrm{dS}=\int_{S_t}(\tau_{ij}u_i+q_j).n_j\,\mathrm{dS} \quad (7)$$

In these equations, p is defined as the pressure, ρ the density, $u_i$the velocity vector, τ_{ij} the viscous stress tensor, E the total energy per unit volume, and q_j the heat flux with the following definitions:

$$\tau_{ij}=2\mu(S_{ij}-\frac{\delta_{ij}}{3}S_{kk}) \quad (8)$$

$$q_j=-k_c\frac{\partial T}{\partial x_j} \quad (9)$$

$$E=\frac{p}{\gamma-1}+\frac{1}{2}u_iu_i \quad (10)$$

Where $S_{ij}=\frac{1}{2}(\frac{\partial u_i}{\partial x_j}+\frac{\partial u_j}{\partial x_i})$ is the strain rate tensor, k_c is the thermal conductivity. The latter are generally functions of the temperature, T.

The viscosity $\mu(T)$ is calculated from Sutherland's law:

$$\mu(t)=T^{3/2}\frac{1+s}{T+s} \quad (11)$$

Here s is a parameter depending on the gas and the temperature range.

It should be noted that since the grid is deformable, the grid velocity with which the surface of a CV is moving is taken into account via u_{gj}. Here, the volume integrals now describe local changes in a CV of variable shape and thus the additional mass and momentum fluxes due to u_{gj}. Since the system of equations given by (1) - (3) is not closed anymore, the unknown grid velocity u_{gj} has to be determined. To compute this grid velocity while considering the conservation principle and avoiding the loss of mass and momentum, the so-called space conservation law (SCL)(Demirdzic and Peric [18]) is applied:

$$\frac{d}{dt}\int_{V_t}\mathrm{dV}+\int_{S_t}u_{gj}.n_j\,\mathrm{dS}=0 \quad (12)$$

3. Numerical schemes

In this section we present the numerical algorithms used to solve the Navier-Stokes equations and moving mesh requirements for a FSI problem. The equations are discretized on an unstructured triangle grid with a finite volume method.

Flux-vector splitting scheme, which has employed in this code, is a advection upstream splitting method AUSM. Here, the flux is split into two separate components so that each one may be properly upwind stencilled. $AUSM$ proposed by Liou and Steffen [19] for 2D Euler equations. In this method the cell interface advection Mach number is appropriately defined to determine the upwind extrapolation for the convective quantities. The flux split into two component: the convective flux term and pressure flux:

$$F_{1/2}=F^c_{1/2}+F^p_{1/2} \quad (13)$$

The convective flux is carried by the flow, i.e. through the entropy wave. It can be defined completely in the upwind direction by using the properties of the convective (entropy) wave. This will be discussed just below. The pressure term of the flux is the term that is carried by the entropy waves, which allow for travel in a direction against the flow in a subsonic situation. This term is to be separated into two relative contributions. First, the convective is shown in Eq. (14).

$$F^c_{1/2}=M_{n_{1/2}}W_{Left\ or\ Right} \quad (14)$$

Where:

$$W = [\rho \quad \rho u \quad \rho v \quad \rho E]^T \tag{١٥}$$

The special Mach number term that has been pulled out of the convective flux term is the "convective" Mach number. The convective Mach number is a measure of the effective convective potential of the flow, based on the strength of the entropy eigenvalue. The convective Mach number can be defined as shown in Eq. (١٦).

$$M_{n_{1/2}} = M_L^+ + M_R^- \tag{١٦}$$

The definition for the left and right Mach numbers were taken from the Van Leer method, as in Eq. (١٧).

$$M^{\pm} = \begin{cases} \pm\frac{1}{4}(M \pm 1)^2 & |M| \le 1 \\ \frac{1}{2}(M \pm |M|) & |M| > 1 \end{cases} \tag{١٧}$$

The "Left or Right" in the remaining flux term is a switch that corresponds to the sign of the convective Mach number. It is defined as follows in Eq. (١٨).

$$W_{Left\ or\ Right} = \begin{cases} W_{Left} & M_{n_{1/2}} \ge 0 \\ W_{Right} & M_{n_{1/2}} < 0 \end{cases} \tag{١٨}$$

The pressure term is treated separately. It is defined so that communication in both directions may be admitted. Eq. (١٩) shows the calculation of the pressure.

$$P^{\pm} = \begin{cases} \frac{P}{4}(M \pm 1)^2(2 \mp M) & |M| \le 1 \\ \frac{P}{2}(1 \pm sign(M)) & |M| > 1 \end{cases} \tag{١٩}$$

The set of partial differential equations Eq. (٥)-(٧) is integrated in time explicitly with a low-storage four-stage Runge-Kutta method which is formally fourth-order accurate for linear equations but drops to second-order accuracy for a general nonlinear equation.

For every control volume, if system of Equations (٥)-(٧) rewrites as:

$$\frac{d}{dt}\boldsymbol{W} + \frac{1}{V}\boldsymbol{R}(\boldsymbol{W}) = 0 \tag{٢٠}$$

Which $\boldsymbol{W}$ refferes to conservative values vector and $R(\boldsymbol{W})$ is residual vector which contains convection and diffusion terms.

Applying a q-stage Runge-Kutta scheme (q≤٥) to the above equation yields:

$$\begin{aligned} \boldsymbol{W}^{\boldsymbol{n+1/q}} &= \boldsymbol{W}^{\boldsymbol{n}} - \beta\varphi_1 \frac{\Delta t}{V}\boldsymbol{R}\left(\boldsymbol{W}^{\boldsymbol{n+0/q}}\right) \\ \boldsymbol{W}^{\boldsymbol{n+2/q}} &= \boldsymbol{W}^{\boldsymbol{n}} - \beta\varphi_2 \frac{\Delta t}{V}\boldsymbol{R}\left(\boldsymbol{W}^{\boldsymbol{n+1/q}}\right) \\ &\vdots \\ \boldsymbol{W}^{\boldsymbol{n+1}} &= \boldsymbol{W}^{\boldsymbol{n}} - \beta\varphi_q \frac{\Delta t}{V}\boldsymbol{R}\left(\boldsymbol{W}^{\boldsymbol{n+(q-1)/q}}\right) \end{aligned} \tag{٢١}$$

Where, $\varphi_1 = 1, \ldots, q$ are the coefficients of the q-stage Runge-Kutta scheme and β the Courant-Friedrichs-Lewy (CFL) number. For a four-stage scheme (q=٤), the coefficients φ_i are:

$$\varphi_1 = \frac{1}{4}, \varphi_2 = \frac{1}{3}, \varphi_3 = \frac{1}{2}, \varphi_4 = 1 \tag{٢٢}$$

In order to capture the boundary layer and the near wake, it is important to maintain a high mesh quality near the moving wing, especially at large deformation problems. Therefore, an accurate mesh motion technique is necessary, which is able to cope with large mesh deformations. So for maintenance the quality of mesh adaption of an accurate and flexible method is needed. In the current work we use RBF interpolation to find the displacements of the internal fluid points for given boundary displacements. The interpolation function $s(\boldsymbol{x})$ describing the displacement of all computational mesh points, is approximated by a sum of basis functions:

$$s(\boldsymbol{x}) = \sum_{j=1}^{N_b} \gamma_j \emptyset \left(\left|\left| \boldsymbol{x} - \boldsymbol{x}_{b_j} \right|\right| \right) + Q(\boldsymbol{x}) \quad (۲۳)$$

Where the known boundary value displacements are given by $\boldsymbol{x}_{b_j} = [x_{b_j}, y_{b_j}, z_{b_j}]$, q is a polynomial, N_b is the number of boundary points and $\emptyset$ is a given basis function as a function of the Euclidean distance $||x||$. The minimal degree of polynomial q depends on the choice of the basis function $\emptyset$ (Boer de et al., [۲۰]). A unique interpolant is given if the basis function$\emptyset$ is a conditionally positive definite function. If the basis functions are conditionally positive definite of order $m \leq ۲$, a linear polynomial can be used (Beckert and Wendland, [۲۱]). We only applied basis functions that satisfy this criterion. A consequence of using a linear polynomial is that rigid body translations are exactly recovered. The polynomial Q is defined by the coefficients γ which can be defined by evaluating the interpolation function $s(x)$ in the known boundary points:

$$s\left(\boldsymbol{x}_{b_j}\right) = \Delta \boldsymbol{x}_{b_j} \quad (۲۴)$$

Here $\Delta \boldsymbol{x}_{b_j}$ contains the known discrete values of the boundary point displacements. Together with the additional requirements:

$$\sum_{j=1}^{N_b} \gamma_j P\left(\boldsymbol{x}_{b_j}\right) \quad (۲۵)$$

Which holds for all polynomials P with a degree less or equal than that of polynomial$Q$, the γ_j values can be determined (Boer de et al., [۲۰]).

The values for the coefficients γ_j and the linear polynomial can be obtained by solving the system:

$$\begin{bmatrix} \emptyset_{bb} & Q_b \\ Q_b & ۰ \end{bmatrix} \begin{bmatrix} \boldsymbol{\gamma} \\ \boldsymbol{\beta} \end{bmatrix} = \begin{bmatrix} \Delta \boldsymbol{x}_{b_j} \\ ۰ \end{bmatrix} \quad (۲۶)$$

where $\boldsymbol{\gamma}$ is containing all coefficients γ_j , $\boldsymbol{\beta}$ the four coefficients of the linear polynomial Q, $\emptyset_{bb}$ an $N_b \times N_b$ matrix contains the evaluation of the basis function $\emptyset_{b_i b_j} = \emptyset \left(\left|\left| \boldsymbol{x}_{b_i} - \boldsymbol{x}_{b_j} \right|\right| \right)$and can be seen as a connectivity matrix connecting allboundary points with all internal fluid points. Q_b is an $N_b \times ۱$ matrix with row j given by$\begin{bmatrix} ۱ & x_{b_j} \end{bmatrix}$.

The additional grid fluxes in the momentum equation have to be consistently determined by applying the SCL in its discrete form denoted discrete geometric conservation laws (DGCL) (Demirdzik and Peric [۱۸]). In the context of the Runge–Kutta time-marching scheme applied in the present study, a consistent numerical formulation reads:

$$\int_{S_c(t)} \rho u_i \left(u_{g.j}\right).n_{j.c}\, dS \approx \sum \rho u_{i,c} \frac{\delta V_c^{n+۱}}{\Delta t} \quad (۲۷)$$

Where δV_c represents the volume swept by the face c during the time step Δt.

٤. Grid and boundary Condition

For problem of the simulation of flow around a flapping foil, an unstructured grid used as "Figure ۱".

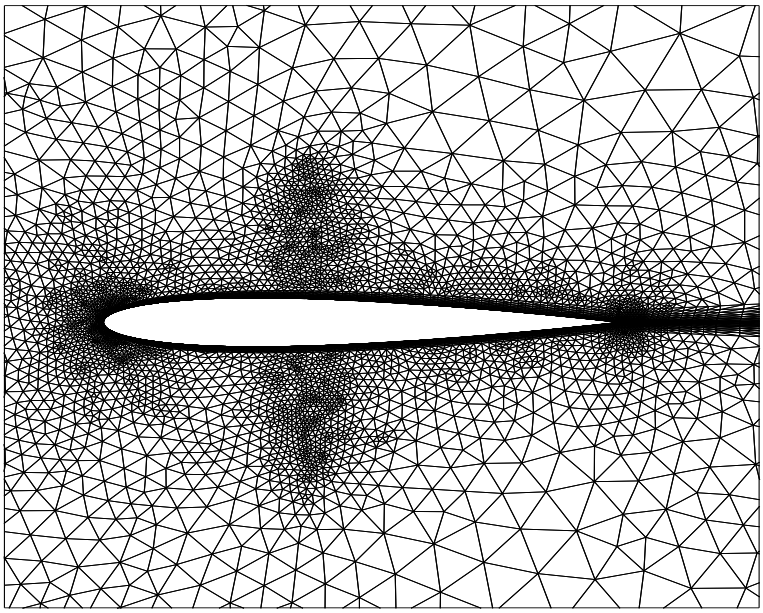

Figure ١. Unstructured Grid used for dividing domain.

This domain has $٣٠c \times ٣٠c$ dimension, which c refers to length of chord. The domain has been divided to ١٧٥٣٦ cells, which is consisted from ٩٠٧٩ node points and ٢٦٤٢٩ face. A steady flow has imposed as inflow and in outflow a subsonic boundary condition has been adopted.

٥. Code validation and verification and results

For validation of the code a benchmark problem has been choose and compared with those obtained by Yu et al. [٢٢]. A two-dimensional case was selected, with a moving wing according to harmonic kinematics. The k was set to ٣٫٥ and $= ٠.٤٥$. Flow regime has considered as a low Reynolds and low Mach Numbers flow with $Re = ١٢٠٠$ and $M_\infty = ٠.١$. Generally, our force distribution looks similar for both cases "Fig٢ ". The instantaneous drag coefficients $cx(t)$, are plotted against Yu's result and the computations were considered to be in good agreement with Yu's. Indeed, the Instantaneous thrust coefficient plot represents the propulsive force which induces with flapping motion.

Maybe with observation of the unsteady inherent of flow pattern in flapping motion, this point be concluded that in comparison with jets or propellers, this type of propulsion could not produce a steady propulsive force, so its flexibility reduces. But it should be noted that the incoming free stream was a steady flow, so unsteadiness of propulsive force does not effect on a steady motion in stream-wise direction. But flapping motion is inherently a accelerated motion.

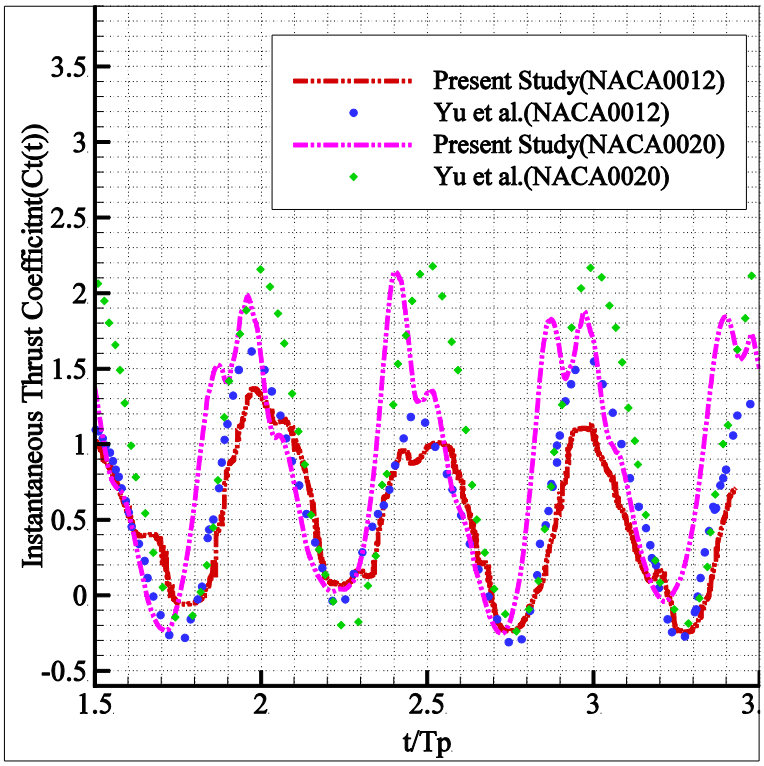

Figure ٢. Comparison of instantaneous thrust coefficient of present study with Yu et al. [٢٢].

In "Figure ٣" snapshots of instantaneous vorticity filed-contour have been plotted. The vorticity pattern is look like flow behind a blunt body. The strength of vorticity in Leading edge region has the maximum magnitude and predicts a suction force in leading edge region (negative dynamic pressure).

In "Figure ٤" mean pressure coefficient on surface of foil has been plotted. It is obvious that: main reason of negative mean pressure coefficient in leading and trailing edge of foil is vortices which form during flapping motion and are cause of propulsion. In "Figure ٢", it seems that a NACA٠٠٢٠ produces more versus NACA٠٠١٢. But "Figure ٤" does not show a large difference between men pressure coefficient of them. The reason of different magnitude of thrust, which produced with each of foils, could be for their different geometry. So geometry of foil could be an effective parameter.

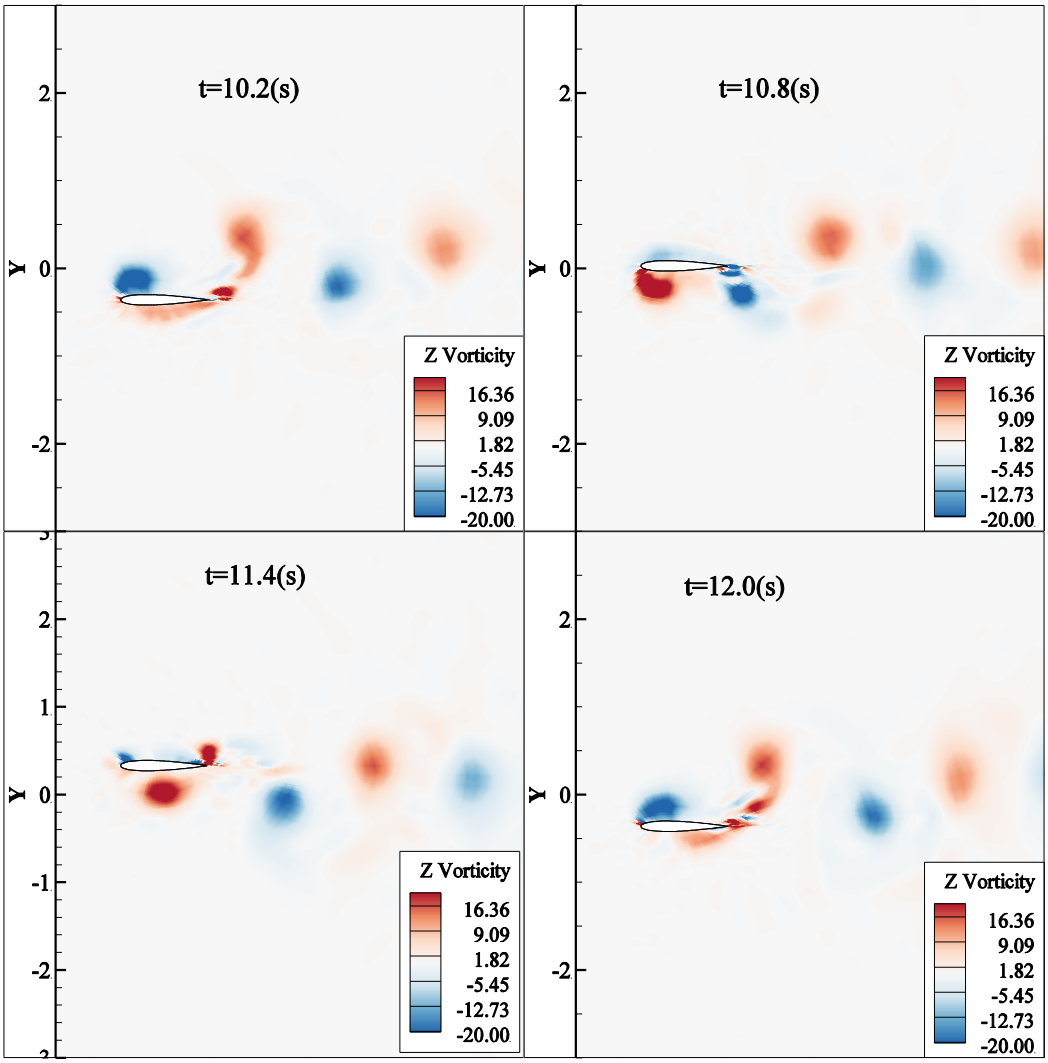

Figure ٣. Instantaneous captured vorticity filed-contour plots with k = ٣,٥; St=٠,٤٥ for a NACA٠٠١٢ foil.

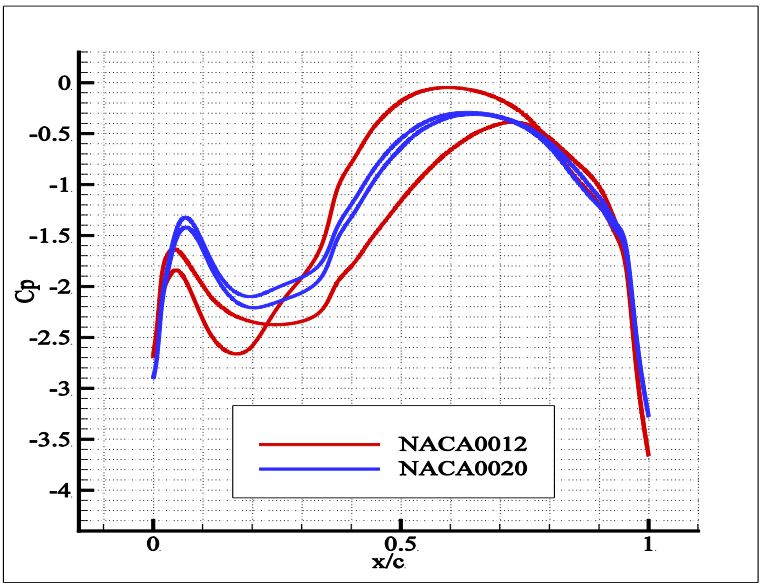

Figure ٤. Comparison of mean pressure coefficient on NACA٠٠١٢ and NACA٠٠٢٠ foil.

"Figure ٥" shows a mean flow pattern. This mean flow achieved by a time averaging procedure during ٢٠ whole period of motion. This mean flow obviously shows the mechanism of thrust generation. Foil operates as a jet.

Discontinuity in velocity magnitude refers to a difference with common jet propulsion systems. The exhausted momentum in a flapping foil is not steady.

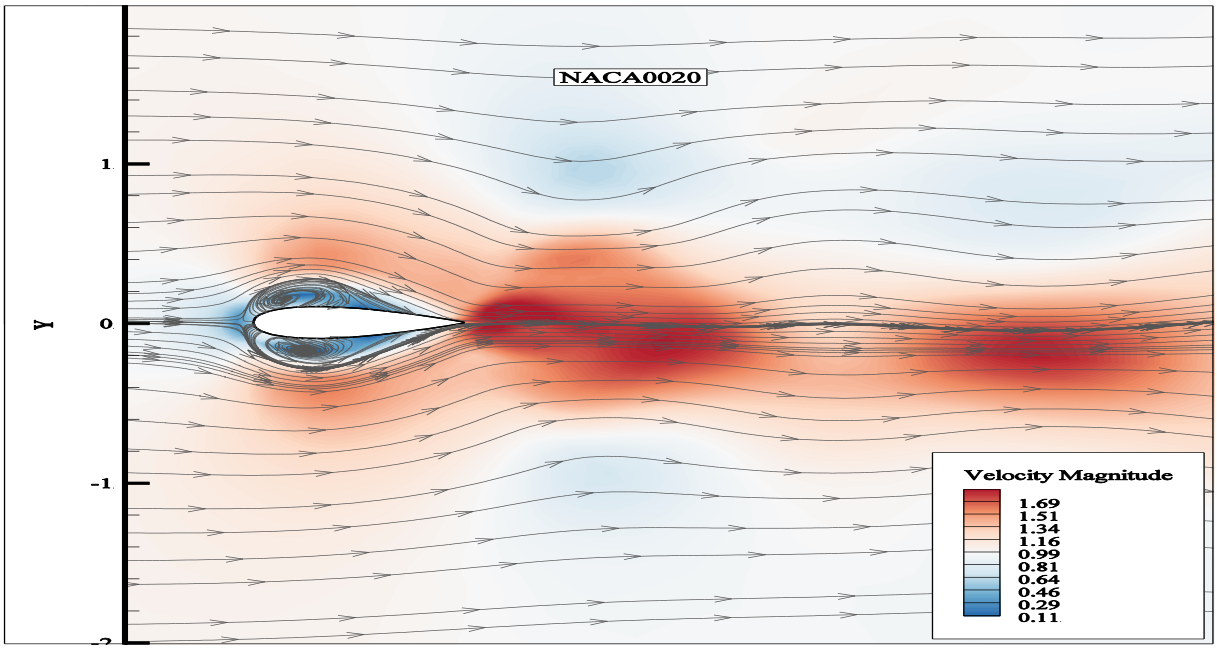

Figure ٥. Streamlines and velocity magnitude of mean flow around a NACA٠٠٢٠ foil.

Conclusions

For simulation of flow at low Reynolds numbers around a flapping foil, a CFD code has been developed. The ability of code verified with evaluation of its result for a benchmark problem. Then flow pattern demonstrated for both instantaneous snapshots and mean flow regime. Leading and trailing edge vortices as main and important factors for produce of propulsive force showed and contribution of pressure coefficient represent that against a fixed foil, a flapping foil is under a suction in leading edge region.

Acknowledgments

The authors gratefully acknowledge the Iranian Society of Computational science and engineering (WWW.Marketcode.ir) for its support.

References

[١] S. Nassef, N. Pornsinsirirak, Y. C. Tai and C. M. Ho, "Unsteady aerodynamics and flow control for flapping wing flyers," *Progress in Aerospace Sciences*, vol. ٣٩, no. ٩, pp. ٦٣٥-٦٨١, ٢٠٠٠.

[٢] M. F. Platzer, K. D. Jones, J. Young and J. C. S. Lai, "Flapping-wing aerodynamics: progress and challenges," *AIAA Journal*, vol. ٤٦, no. ٩, pp. ٢١٣٦-٢١٤٩, ٢٠٠٨.

[٣] K. V. Rozhdestvensky and V. A. Ryzhov, "Aerohydrodynamics of flapping-wing propulsors," *Progress in Aerospace Sciences*, vol. ٣٩, no. ٨, pp. ٥٨٥-٦٣٣, ٢٠٠٣.

[٤] W. Shyy, H. Aono, S. Chimakurthi, P. Trizila, C. Kang, C. Cesnik and H. Liu, "Recent progress in flapping wing aerodynamics and aeroelasticity," *Progress in Aerospace Sciences*, vol. ٤٨, no. ٧, pp. ٢٨٤-٣٧٢, ٢٠١٠.

[٥] R. Knoller, "Die Gesetze des Luftwiderstandes," *Flug- und Motortechnik*, vol. ٣, no. ٢١, pp. ١-٧, ١٩٠٩.

[٦] A. Betz, "Ein Beitrag zur Erklaerung des Segelfluges," *Zeitschrift fur Flugtechnik und Motorluftschiffahrt*, vol. ٣, pp. ٢٦٩-٢٧٢, ١٩١٢.

[٧] R. Katzmayr, "Effect of periodic changes of angle of attack on behavior of airfoils," National Advisory Committee for Aeronautics, Washington DC, ١٩٢٢.

[٨] T. Von Karman and J. M. Burgers, Aerodynamic Theory: A General Review of Progress, ١٩٣٥.

[٩] P. Freymuth, "Propulsive vortical signature of plunging and pitching airfoils," *AIAA Journal*, vol. ٢٦, pp. ٨٨١-٨٨٣, ١٩٨٨.

[١٠] M. M. Koochesfahani, "Vortical patterns in the wake of an oscillating airfoil," *AIAA Journal*, vol. ٢٧, pp. ١٢٠٠-١٢٠٥, ١٩٨٩.

[۱۱] G. S. Triantaflyllou, M. S. Triantaflyllou and M. A. Grosenbaugh, "Optimal thrust development in oscillating foils with application to fish propulsion," *Journal of Fluids and Structures,* vol. ۷, pp. ۲۰۵-۲۲٤, ۱۹۹۳.

[۱۲] K. D. Jones, C. M. Dohring and M. F. Platzer, "Experimental and computational investigation of the Knoller–Betz effect," *AIAA Journal,* vol. ۳٦, pp. ۱۲٤۰-۱۲٤٦, ۱۹۹۸.

[۱۳] J. C. S. Lai and M. F. Platzer, "Jet characteristics of a plunging airfoil," *AIAA Journal,* vol. ۳۷, pp. ۱۵۲۹-۱۵۳۷, ۱۹۹۹.

[۱٤] Z. J. Wang, "Vortex shedding and frequency selection in flapping flight," *Journal of Fluid Mechanic,* vol. ٤۱۰, pp. ۳۲۳-۳٤۱, ۲۰۰۰.

[۱۵] J. Young and J. C. S. Lai, "Oscillation frequency and amplitude effects on the wake of a plunging airfoil," *AIAA Journal,* vol. ٤۲, pp. ۲۰٤۲-۲۰۵۲, ۲۰۰٤.

[۱٦] T. Schnipper, A. Andersen and T. Bohr, "Vortex wakes of a flapping foil," *Journal of Fluid Mechanic,* vol. ٦۳۳, pp. ٤۱۱-٤۲۳, ۲۰۰۹.

[۱۷] D. G. Bohl and M. M. Koochesfahani, "MTV measurements of the vertical field in the wake of an airfoil oscillating at high reduced frequency," *Journal of Fluid Mechanic,* vol. ٦۲۰, pp. ٦۳-۸۸, ۲۰۰۹.

[۱۸] I. Demirdzic and M. Peric, "Space Conservation Law In Finite Volume Calculations Of Fluid Flow," *International Journal For Numerical Methodes In Fluids,* vol. ۸, pp. ۱۰۳۷-۱۰۵۰, ۱۹۸۸.

[۱۹] M. Liou and C. Stefen, "A New Flux Splitting Scheme," *Journal of Computational Physics,* vol. ۱۰۷, pp. ۲۳-۳۹, ۱۹۸۱.

[۲۰] A. Boer de, M. S. van der Schoot and H. Bijl, "Mesh deformation based on radial basis function interpolation," *Computers and Structures* , vol. ۸۵, p. ۷۸٤–۷۹۵, ۲۰۰۷.

[۲۱] A. Beckert and H. Wendland, "Multivariate interpolation for fluid-structure-interaction problems using radial basis functions," *Aerospace Science and Technology* , vol. ۵, no. ۲, p. ۱۲۵–۱۳٤, ۲۰۰۱ .

[۲۲] M. Yu, Z. J. Wang and H. Hu, "Airfoil Thickness Effects on the Thrust Generation of Plunging Airfoils," *JOURNAL OFAIRCRAFT,* vol. ٤۹, pp. ۱٤۳٤-۱٤۳۹, ۲۰۱۲.